國 立 交 通 大 學

電信工程研究所

碩 士 論 文

於60Ghz無線電傳輸下的空時前置編碼混合式波束成形架構及基於方向的前置編碼器碼書設計

A Space-Time Precoded Hybrid Beamforming Architecture with Direction-Based Precoder Codebook Design in 60Ghz Radio

研究生：殷裕雄

指導教授：伍紹勳

中 華 民 國 100 年 9 月 13 日

於 60Ghz 無線電傳輸下的空時前置編碼混合式波束成形架構及基於方向的前置編碼器碼書設計

A Space-Time Precoded Hybrid Beamforming Architecture with Direction-Based Precoder Codebook Design in 60Ghz Radio

研 究 生：殷裕雄　　Student：Yu-Hsiung Yin

指導教授：伍紹勳　　Advisor：Sau-Hsuan Wu

國 立 交 通 大 學
電 信 工 程 研 究 所
碩 士 論 文

A Thesis
Submitted to Institute Communications Engineering
College of Electrical and Computer Engineering
National Chiao Tung University
in partial Fulfillment of the Requirements
for the Degree of
Master
in
In

Communications Engineering

October 2011

Hsinchu, Taiwan, Republic of China

中華民國一百年十月

於 60Ghz 無線電傳輸下的空時前置編碼混合式波束成形架構及基於方向的前置編碼器碼書設計

學生：殷裕雄　　　　　　　　　　　　　　　　指導教授：伍紹勳

國立交通大學電信工程研究所碩士班

摘　　　要

在 60Gh 無線電傳輸下，探討使用平面貼片天線陣列、混合式射頻及基頻波束成形技術的一個有效率的架構。在此架構下，一個具備空時及前置編碼的混合式波束成形架構被用來有效利用在 60Ghz 無線電傳輸下非直視路徑傳輸造成的空間分歧性。此外，一個有效率的單位元迴饋波束成形架構被提出來找出能夠支援直視路徑傳輸、最適合射頻波束成形所打的方向。模擬結果顯示提出的混合式波束成形架構相對於射頻波束成形架構能在訊號雜訊比上了提供 5~10db 的增益。此外，使用基於方向設計的前置編碼器碼書及單位元迴饋波束成形機制的效能在 100 次遞迴次數內收斂接近於直視路徑的效能，顯示出其遠比利用窮舉法的搜尋方式有效率的優點。此外，在對前置編碼器量化的情況下，使用提出的前置編碼器碼書的效能與未對前置編碼器量化的效能相當接近。

A Space-Time Precoded Hybrid Beamforming Architecture with Direction-Based Precoder Codebook Design in 60Ghz Radio

Student：Yu-Hsiung Yin Advisors：Dr. Sau-Hsuan Wu

Institute of Communications Engineering
National Chiao Tung University

ABSTRACT

A cost-effective architecture is studied for a joint radio frequency (RF) and baseband hybrid beamforming (HBF) method that uses planar antenna arrays (PAA) in 60GHz radio transmission. Under the hybrid architecture, a space-time precoded HBF scheme is presented to exploit the spatial diversity for non line-of-sight transmission in 60GHz radio. Furthermore, an efficient one-bit feedback (OBF) beamforming (BF) scheme combined with direction-based precoder codebook design criterion is proposed to search for the pointing directions of each RF beamformer (BFer) of the HBF architecture. Simulation results show that the proposed HBF architecture can provide a 5 ~ 10dB gain in the signal to noise ratio compared to an architecture that uses the RF BF only. In addition, the OBF BF scheme with the direction-based precoder codebook converges close to the LOS transmission in 100 iterations, which is much more efficient than exhaustively searching for the BF directions. With the quantization of optimal precoder utilizing the proposed precoder codebook, the performance is similar to that of the optimal precoder without quantization.

誌　　謝

感謝我的指導教授伍紹勳老師兩年來的指導，從老師身上學到的不止是研究的學問，更重要的是那份嚴謹的態度及追根究底的精神。

感謝MBWCL的學長姐，給予我在課業及生活上的幫助。尤其是博士班學長邱麟凱，對於我的研究及計劃花費相當大的心力，謝謝你們從旁給予我的協助，並且讓我在你們身上學習到做研究應有的態度及學問。感謝MBWCL的同學與學弟，不時地給我幫助和鼓勵。同學們一起修課時互相照應、生活中互相扶持、水深火熱拼進度時互相加油打氣，我不會忘記那些星期五晚上聚在薑母鴨的日子。

感謝我的爸媽及哥哥，謝謝你們的呵護和體諒，支持我並讓我能無後顧之憂地完成碩士生涯。當然我要感謝我的女朋友，在我忙得不可開交時細心地照顧我、在我面臨低潮時為我打氣。

最後，我要感謝交通大學。大學和研究所的六年—交大電信系、交大通訊所，謝謝這個讓我茁壯的環境。

謹此致上最誠摯的謝意

誌於 2011.10 新竹 交通大學

裕雄

Contents

List of Figures

Chapter 1

Introduction

The increasing demands on the bandwidth for personal and indoor wireless multimedia applications have driven the research and development for a new generation of broadband wireless personal area network (WPAN) [1]. The characteristics of broad unlicensed bandwidth, high penetration loss and significant oxygen absorption [2] at 60GHz radio make it an ideal wireless interface to support spatial reuse in the next generation WPAN. On the contrary, to provide high data rates for local users under the severe penetration and path losses, beamforming (BF) emerges as an important technology to support high directivity in 60GHz radio transmission.

In many standards of 60Ghz radio [1, 3, 4], planar antenna array (PAA) has been adopted to improve the system performance. The low profile, low fabrication cost with printed circuit techniques, simple linear, circular or dual polarization, easy fabrication into linear arrays and easy integration with the microwave circuits properties of microstrip patch antenna make it a suitable option to construct the antenna array in mmWave radio [5]. Due to the tiny size of patch antenna in 60Ghz mmWave radio, large scale array is acceptable which makes it feasible to use tens of tiny antennas to steer the radio signal. The resultant large array gain can compensate the severe path loss and high directivity can not only increase the spatial reuse degree but also reduce the severe multipath effect [6]. In the PAA, each patch antenna is equipped with a phase shifter. By adjusting the phase shifters, the transmitter can control the direction of constructive interference and form the radio frequency beamforming (RF BF). The main lobe of the beam pattern is called the pointing direction of the transmit antenna.

With the BF scheme, system performance is determined by the pointing direction significantly. To truly benefit from the high-directivity beamformed radio signal, correct information for the angle of departure (AoD) of the signal plays an important role in transmission. With the beamforming scheme, the pointing direction align with the line-of-sight (LOS) path results in LOS transmissions. When the LOS path is not blocked, intuitively, having the beam direction of each block pointed to the receiver can improve the received signal quality with LOS transmissions in Fig. 1.1. When the LOS path is blocked, beamforming with the pointing direction toward the best reflection path has better performance than other paths in Fig. 1.1. If the transmitter knows the user direction, intuitively, beamforming with the pointing direction toward the user direction achieves the optimal performance. However, the direction of the receiver is often not provided *a priori* to the transmitter. Besides, transmissions may also be blocked by obstructions as illustrated in Fig. 1.3. Therefore, an effective algorithm to search for the appropriate RF beam directions is crucial to the success of the BF scheme in 60GHz radio. There are some researches on such beam steering issue. First one is the codebook-based beamforming [7] which is operated in the media access control (MAC) layer for the directional antenna and has been adopted in [1]. It aims at searching for the optimal pointing direction for RF beamformer (BFer). Another one is the distributed one-bit feedback beamforming [8, 9]. This kind of research aims at searching for the beamforming weights to compensate the effect of the Rayleigh fading channel in the physical layer. Compared with the above researches, we propose a beam steering algorithm for directional antenna operated in the physical layer to reduce the transmission time for the MAC layer design.

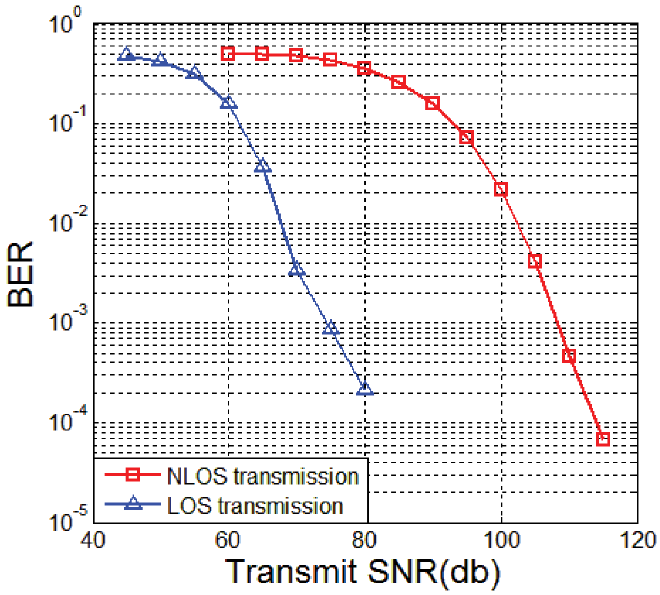

Figure 1.1: Performance comparison in BER between the LOS and NLOS transmission when the LOS path is not blocked.

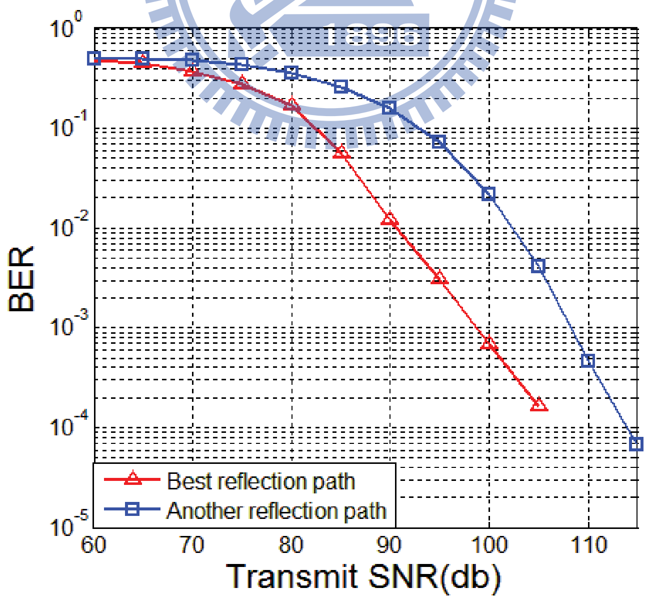

Figure 1.2: Performance comparison in BER between the pointing direction toward the best reflectional path and another reflection.

Considering the implementation cost of a full digital baseband BF technique with PAA, we adopt the PAA structure proposed in [10] which partitions the element antennas of the PAA into blocks. The element antennas in the same block are driven by a common baseband digital signal to form the hybrid beamforming which is combined with the RF BF and baseband BF. The equivalent baseband transmission system can be considered as a multiple input single output (MISO) system such that it is able to apply the baseband signal processing, such as space time code (STC) or precoding, to the transmission. Applications such as angle of arrival (AoA) detection at the receiver [11], MIMO precoder scheme in the WirelessHD standard [4] and power minimization for two user spatial division multiple access (SDMA) [12] use similar HBF architecture to improve the system performance in millimeter wave radio.

Considering that when the LOS path is blocked or user direction is unknown to the transmitter, the system may have NLOS transmissions. Conventionally, STC techniques such as the Alamouti scheme [13] have been adopted at the transmitter to exploit the diversity under the NLOS transmission, and thus improve the error probability under the fading channel. Such STC scheme, however, can be further enhanced by adapting to the channel conditions with the precoding techniques. If a high rate feedback link is unavailable, it is possible to limit the adaption to the channel statistics which are by nature slow varying in mmWave radio [14]. Channel statistics convey important spatial information about antenna correlation, mean and the standard deviation of angles of departure (AoD) or AoA, which can be exploited in the design of a precoder matrix so as to minimize the error rate, such as symbol error rate [15,16] and pairwise error probability [17–19], or maximize mutual information [20]. Besides, the channel is dominated by a relatively small number of paths which results in the severe frequency selective fading [21]. We thus use the orthogonal frequency division multiple (OFDM) system to overcome the multipath effect. There have been some researches on the precoded MIMO OFDM system [22] and space time precoded MIMO OFDM system [23]. However, we propose a space time precoded hybrid beamforming (ST-precoded HBF) architecture with OFDM system especially in millimeter wave radio.

Channel characteristics for highly directional 60Ghz links differ significantly [21]. Different pointing directions of the RF beam patterns may result in different channel characteristics, such as channel mean and spatial correlation, observed in the baseband [24]. Such phenomenon raises the issue of precoder codebook design to support the transmission with various channel statistics in millimeter wave radio. Early ideas behind limited feedback linear precoding focused on quantizing the channel matrix [25] where the receiver would quantize the channel, feed back the quantized value to the transmitter, and then have the transmitter pick the precoder assuming that this quantized side information is the perfect channel realization. Such ideas fundamentally do nothing more than allowing the receiver to design the precoder matrix directly and send it back to the transmitter, the problem could be approached differently as one of precoder codebook designs rather than channel codebook design. In this kind of researches, [26] and [27] proposed the Grassmannian line packing (GLP) criterion for the precoder codebook with a spatially uncorrelated and correlated Rayleigh fading channel respectively, and [28] proposed a codebook design criterion with the techniques of vector quantization (VQ). However, these design criteria usually consider only that the channel statistics is invariant which is not the case when the channel statistics varies along with the changing of pointing directions of the transmit antennas in millimeter wave radio. Thus, a precoder codebook adaptive to the various channel statistics which is resulted from the different pointing directions is much essential in the ST-precoded HBF architecture.

One method for designing precoder codebook satisfying this demand is that the receiver collects all the channel statistics of adjustable pointing directions and then design the associated precoder codebook and send it back to the transmitter. Apparently, once the indoor environment changes, the receiver must repeat the collecting and feedback procedure which leads to the large overheads for channel measurement and feedback.

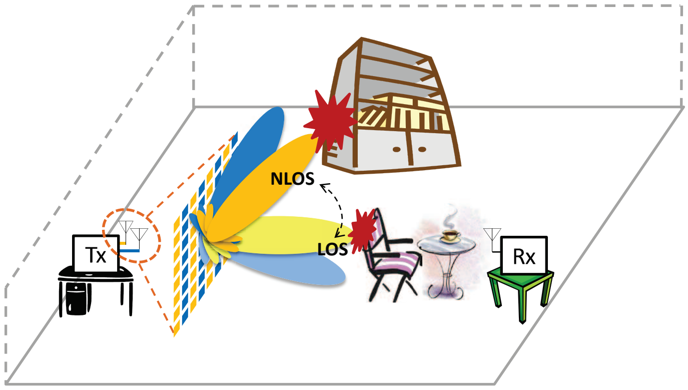

Figure 1.3: Overall 2 × 1 system scheme. Antenna arrays of 8 × 8 planar antennas. Patch antennas in different colors belong to different blocks.

Thus, we propose a precoder codebook design method at both the transmitter and receiver in which the receiver doesn't require to feedback the codebook to the transmitter every time when the indoor environment changed which reduces the overheads significantly.

In view of the importance of BF for 60Ghz radio, we present herein a cost-effective beam steering algorithm jointly with the precoder codebook design for the proposed ST-precoded HBF architecture using PAA. Based on the one-bit feedback (OBF) BF techniques [8,9,29], we develop an iterative approach to search for the appropriate beam direction for each one of the antenna blocks of the PAA. The ST precoding method in [19] is employed to exploit the statistical baseband channel side information at the transmitter (CSIT) to further improve the system performance. At each iteration of the proposed beam steering algorithm, the precoder codebook is constructed with the corresponding channel characteristics resulted from the pointing directions concurrently. Given that the receiver can estimate the channel state information (CSI), pair-wise error probability (PEP) of the precoder is used as the predicted metric to choose the optimal precoder codeword for the current pointing direction from the corresponding codebook. In the end of the OBF procedure the transmitter can transmit data streams toward the optimal direction with the associated optimal precoder in the codebook.

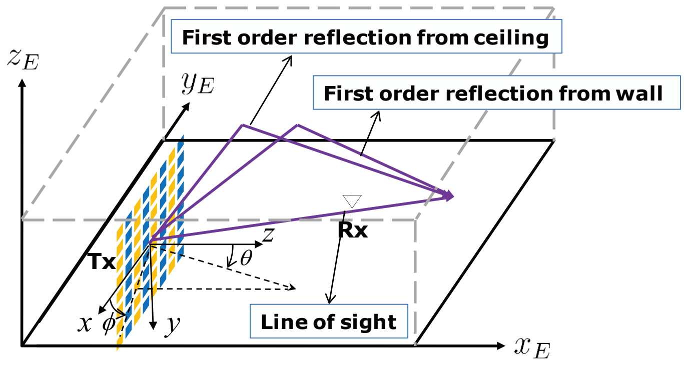

Figure 1.4: Indoor conference environment. HBF architecture and single onmi-directional antenna are used at the transmitter and receiver respectively which forms the equivalent MISO baseband channel. The receiver may receive signals from the LOS path or reflection path from the wall or ceiling

According to the simulation results, the diversity order of the baseband channel can be effectively increased with the proposed HBF scheme in non LOS (NLOS) transmissions. In addition,the proposed ST-precoded HBF scheme provides about 2∼ 4 db precoding gain in BER under LOS transmissions. The convergence curves in PEP upper bound shows that the performance of LOS transmission can be approached by the OBF algorithm in 100 iterations, and the performance between the OBF algorithm with and without the quantization of optimal precoder is just a modicum.

Notations: In this paper, we use lowercase letters, e.g., a, to represent scalars, bold-faced lowercase letters, e.g., **a**, to represent vectors and uppercase letters, e.g., **A**, to represent matrices. vec(·) stands for concatenating the columns of the matrix argument into a vector. $[\mathbf{A}]_i$ stands for the i-th column of matrix **A**. $\|\cdot\|$ represents the Frobenius norm. The superscipts '$\dagger$' and '-1' represent Hermitian transpose and inverse of matices. The superscipt '$*$' stands for complex conjugate of the scalar. The notations $\mathbb{C}^{i\times j}$ and $\mathbb{R}^{i\times j}$ represent the sets of i×j-dimentional complex and real matrices. For simplicity, $\forall i, j \in \mathcal{N}$, where $\mathcal{N}$ stands for the natural number.

Chapter 2

60GHz Indoor Channel Model for PAAs

To investigate the performance of the proposed ST-precoded HBF architecture and associated beam steering algorithm with precoder codebook design in 60GHz radio, the baseband channel is simulated with the measurement results reported in [3] for a typical conference room 1.4. According to [3], the baseband channel between the i-th transmit antenna and receive antenna which is a multi-path Rician fading channel can be simply expressed as

$$h^{(i)}(\tau) \triangleq \frac{1}{\sqrt{L+1}}\mathcal{L}_0 G_0^{(i)} a_0^{(i)} \delta(\tau) + \frac{1}{\sqrt{L+1}} \sum_{l=1}^{L} \mathcal{L}_l G_l^{(i)} a_l^{(i)} \delta(\tau - \tau_l) \quad (2.1)$$

where L is the number of multi-path. For $l \neq 0$, the l-th path which occurs due to the reflection has the path loss $\mathcal{L}_l$, the antenna gain from the i-th transmit antenna $G_l^{(i)}$, the time delay τ_l, and complex Gaussian distributed coefficient $a_l^{(i)}$ with zero mean and unit variance for the i-th transmit antenna. The similar notations with sub-index "0" in (2.1) correspond to the LOS while $a_0^{(i)}$ is a complex constant with magnitude equal

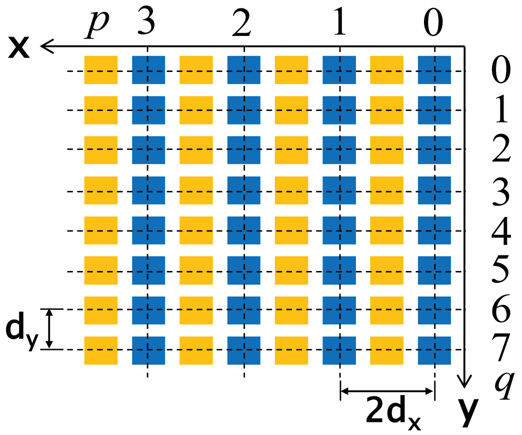

Figure 2.1: PAA configuration for HBF architecture.

to 1.

Based on the axis defined in 1.4, the configuration of PAA is shown in 2.1 where each block of the PAA is an equivalent transmit antenna, the transmit antenna gain of the i-th equivalent transmit antenna is the product of antenna pattern of patch antenna $E(\phi, \theta)$ and the RF BF pattern of the i-th block $A^{(i)}(\phi, \theta)$ [30]. Therefore, the transmit antenna gain for the l-th path from the i-th transmit antenna in this paper is defined as

$$G_l^{(i)} = A^{(i)}(\phi_l, \theta_l) E(\phi_l, \theta_l) = f_G(\hat{\phi}_i, \hat{\theta}_i),$$

where ϕ_l and θ_l are the AoD in the azimuth and elevation. $\hat{\phi}_i$ and $\hat{\theta}_i$ are the pointing direction in azimuth and elevation angles respectively for the RF BF of the i-th transmit antenna. For directional antenna, the antenna gain is determined by the pointing direction significantly. Therefore, it is notable that the channel is affected by the pointing direction of the RF BF in millimeter wave radio with PAA. The detail expression of the antenna pattern of the patch antenna can be found in [12], and the RF BF pattern of the i-th transmit antenna can be expressed as

$$A^{(i)}(\phi, \theta) = \sum_{p=0}^{3} \sum_{q=0}^{7} e^{j[2p(\Psi_x(\phi,\theta)+\alpha_x^{(i)})+q(\Psi_y(\phi,\theta)+\alpha_y^{(i)})]} \tag{2.2}$$

with $\alpha_x^{(i)} = \frac{2\pi}{\lambda} d_x \sin\hat{\theta}_i \sin\hat{\phi}_i$, $\alpha_y^{(i)} = \frac{2\pi}{\lambda} d_y \sin\hat{\theta}_i \cos\hat{\phi}_i$, $\Psi_x(\phi,\theta) = \frac{2\pi}{\lambda} d_x \sin\theta \sin\phi$ and $\Psi_y(\phi,\theta) = \frac{2\pi}{\lambda} d_y \sin\theta \cos\phi$ when the coupling effect among element antennas is neglected. λ is the wave length and d_x and d_y are the distance between two adjacent element antennas of the PAA in x-direction and y-direction, respectively . From (2.1) and (2.2), we can know that the changing of the pointing direction in the RF BF influences the baseband channel although there is no changing of the environment. In this paper, we consider the situation that the pointing direction of the RF BF is chosen from the finite set due to the practical limitation of finite resolution in phase shifters used in PAA, and we assume that the finite resolution in phase shifters restricts the available pointing directions for the RF BF belong to the sets of

$$\begin{aligned} \hat{\theta}_i &\in \left\{0, \frac{\pi}{8}, \frac{2\pi}{8}, \frac{3\pi}{8}, \frac{4\pi}{8}\right\} \\ \hat{\phi}_i &\in \left\{\frac{\pi}{8}, \frac{2\pi}{8}, \frac{3\pi}{8}, \frac{4\pi}{8}, \frac{5\pi}{8}, \frac{6\pi}{8}, \frac{7\pi}{8}, 0\right\}. \end{aligned} \tag{2.3}$$

Chapter 3

Baseband System Model

The baseband system architecture is shown in Fig. 3.1. To overcome the severe multi-path channel effects in 60GHz radio, orthogonal frequency division multiplexing (OFDM) is used for transceiving. Let S_p, $p \in \mathcal{N}$, be the modulated symbols. The codeword of the Alamouti STC [13] expressed as

$$\mathbf{C}_p = \begin{bmatrix} S_{2p-1} & S_{2p}^* \\ S_{2p} & -S_{2p-1}^* \end{bmatrix} \tag{3.1}$$

Due to the rich frequency selectivity in 60Ghz channels, the channels of the neighboring tones might not be similar enough. However, in contrast, the channels of two adjacent OFDM symbols are likely due to the slowly temporal variation property in

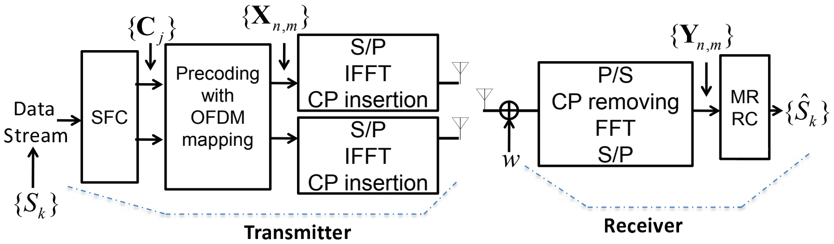

Figure 3.1: The transmitter and receiver architecture of the 2×1 MISO OFDM system.

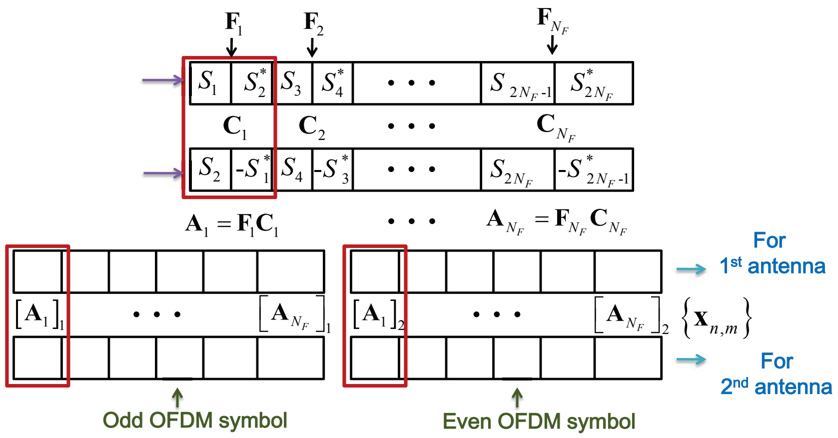

Figure 3.2: Precoding works on the same tone of adjacent OFDM symbols. This figure shows the precoding operations for the first two OFDM symbols.

60Ghz channels with the coherent time about $3ms$ [14]. The STC codewords are then sent to the precoding scheme where the same tone of each two adjacent OFDM symbols has its own precoder working on the corresponding STC codeword.

Let $\mathbf{x}_{n,m}$, for $m \in \mathcal{N}$ to be the transmitted symbol of the n-th frequency tone where $n = 1, \ldots, N_F$ in the m-th OFDM symbols. The 2×1 vector, $\mathbf{x}_{n,m}$, for $m = 2i$ and $m = 2i - 1$ can be expressed as

$$\begin{aligned} \mathbf{x}_{n,2i-1} &= [\mathbf{A}_{(i-1)N_F+n}]_1, \\ \mathbf{x}_{n,2i} &= [\mathbf{A}_{(i-1)N_F+n}]_2 \end{aligned} \tag{3.2}$$

where

$$\mathbf{A}_{(i-1)N_F+n} = \mathbf{F}_{n,i}\mathbf{C}_{(i-1)N_F+n} \tag{3.3}$$

is the product of the precoding matrix, $\mathbf{F}_{n,i}$, of the n-th tone for the $2i - 1$ and $2i$ OFDM symbols and the STC codewords, and $[\mathbf{A}_i]_q$ stands for the q-th column of the 2×2 matrix $\mathbf{A}_i$. In other words, the precoded symbols are seperated into the same tone of neighboring OFDM symbols, which is shown in Fig.3.2.

The received signal of the n-th frequency tone in the m-th OFDM symbol can be expressed as

$$y_{n,m} = \mathbf{h}_{n,m}\mathbf{x}_{n,m} + w_{n,m} \tag{3.4}$$

where $w_{n,m} \sim \mathcal{C}N(0, \sigma_w^2)$ and the channel matrix $\mathbf{h}_{n,m}$, which is a 1×2 row vector, is assumed to be perfectly known at the receiver but not known at the transmitter as *a priori*. The receiver performs maximum-likelihood (ML) detection over a codeword to obtain the

$$\hat{S}_p = arg \min_{\mathbf{x}} \|y - \mathbf{hx}\| \tag{3.5}$$

The mapping in (3.2) allows us to operate the precoding and STC across two adjacent OFDM symbols and to obtain the best performance of the Alamouti code when the channel matrices of the n-th frequency tone in two adjacent OFDM symbols, $m = 2i$ and $m = 2i - 1$, are the same.

Chapter 4

Precoding scheme

High rate feedback link is often not available for the precoding scheme in millimeter wave radio. Considering the phenomenon of channel fading and the delay in CSIT acquisition, precoding based on partial CSIT such as channel statistics may be more realistic than based on the instantaneous CSI when there exists only low rate feedback link.

In 60Ghz radio, the channel mean reponds to the LOS or NLOS transmission which affects the system performance significantly. Besides, transmit correlation resulted from HBF architecture and NLOS transmissions also degrades the link quality. Therefore, we would use the channel mean and transmit correlation as the channel statistics for precoding to further improve the system performance in the ST-HBF scheme. The transmit correlation matrix, $\mathbf{R}_{n},$, is defined by a 2×2 matrix

$$\mathbf{R}_n \triangleq \mathbb{E}[\mathbf{h}_{n,m}^{\dagger}\mathbf{h}_{n,m} - \overline{\mathbf{h}}_n^{\dagger}\overline{\mathbf{h}}_n] \tag{4.1}$$

which stands for the transmit correlation matrix of the n-th frequency tone.

Considering that the channel statistics of each tone are different to each other due to the severe multipath effect, one may use the precoding working on each tone, that is, each tone has its own precoder to deal with the corresponding STC codeword. This method is denoted by precoding scheme using Type.I estimator where the estimates are are obtained by taking the average on N_T time samples

$$\overline{\boldsymbol{\mathcal{H}}}_{T,n} = \frac{1}{N_T}\sum_{m=1}^{N_T}\mathbf{h}_{n,m} \tag{4.2}$$

$$\boldsymbol{\mathcal{R}}_{T,n} = \frac{1}{N_T}\sum_{m=1}^{N_T}(\mathbf{h}_{n,m} - \overline{\boldsymbol{\mathcal{H}}}_{T,n})^{\dagger}(\mathbf{h}_{n,m} - \overline{\boldsymbol{\mathcal{H}}}_{T,n}). \tag{4.3}$$

As a result, the estimates vary with the frequency tones. Such method, however, results in the huge oveheads for computing and and feedbacking the numerous precoder matrices. A design criterion based on the best average performance on all tone is thus required. In this case, the estimates are obtained by taking average over the frequency tones within the r-th OFDM symbol is called Type II estimator. Therefore, we have

$$\overline{\boldsymbol{\mathcal{H}}}_{F} = \frac{1}{N_F}\sum_{n=1}^{N_F}\mathbf{h}_{n} \tag{4.4}$$

$$\boldsymbol{\mathcal{R}}_{F} = \frac{1}{N_F}\sum_{n=1}^{N_F}(\mathbf{h}_{n} - \overline{\boldsymbol{\mathcal{H}}}_{F})^{\dagger}(\mathbf{h}_{n} - \overline{\boldsymbol{\mathcal{H}}}_{F}) \tag{4.5}$$

for all frequency tones. The third one is called Type III which uses the identity matrix to replace the transmit correlation matrix, i.e., $\boldsymbol{\mathcal{R}} = \mathbf{I}$, and (4.4) for the channel mean.

Combining the STC scheme, pairwise error probability (PEP) averaging on channel samples satisfies the demands and is suitable for being the performance metric with above estimators.Regarding that packet error rate is commonly adopted as a design rule to evaluate a space time coded system [31] which is obtained by averaging the channel samples, we use the the upper bound of the PEP with the precoder as the performance metric to design precoder and track the best direction for RF BFer based on the concept of OBF in this section.

Given the mean and the transmit correlation of the channel, we adopt a design criterion in [19] that minimizes the PEP of precoding in HBF.

Suppose that the distribution of $\mathbf{h}_{n,m}$ is given by

$$g(\mathbf{h}_{n,m}) = \frac{\exp(-\mathrm{tr}\left[(\mathbf{h}_{n,m} - \overline{\boldsymbol{\mathcal{H}}})^\dagger \boldsymbol{\mathcal{R}}^{-1}(\mathbf{h}_{n,m} - \overline{\boldsymbol{\mathcal{H}}})\right])}{\pi^2 \det(\boldsymbol{\mathcal{R}})} \tag{4.6}$$

The PEP, which is the probability that a STC codeword $\mathbf{C}_{(i-1)N_F+n}$ is detected as another codeword $\hat{\mathbf{C}}_{(i-1)N_F+n}$, can be upper bounded by

$$\begin{aligned} & P(\mathbf{C}_{(i-1)N_F+n} \to \hat{\mathbf{C}}_{(i-1)N_F+n}) \\ \leq \; & \mathbb{E}_{\mathbf{h}_{n,2i}}[\exp(-\frac{\rho_R}{4}\mathrm{tr}(\mathbf{h}_{n,2i}\mathbf{F}_{n,i}\mathbf{D}\mathbf{F}_{n,i}^\dagger \mathbf{h}_{n,2i}^\dagger))] \\ = \; & \frac{\det(\boldsymbol{\mathcal{R}})}{\det(\mathbf{W}_{n,i})} \exp\left(\mathrm{tr}\left[\overline{\boldsymbol{\mathcal{H}}}(\mathbf{W}_{n,i}^{-1} - \boldsymbol{\mathcal{R}}^{-1})\overline{\boldsymbol{\mathcal{H}}}^\dagger\right]\right) \\ \triangleq \; & \varepsilon(\rho_R, \boldsymbol{\mathcal{R}}, \overline{\boldsymbol{\mathcal{H}}}, \mathbf{F}_{n,i}) \end{aligned} \tag{4.7}$$

where $\mathbf{h}_{n,2i} = \mathbf{h}_{n,2i-1}$ is assumed. $\overline{\boldsymbol{\mathcal{H}}}$ and $\boldsymbol{\mathcal{R}}$ are normalized estimators on channel mean and transmit correlation satisfing

$$\mathrm{tr}\{\overline{\boldsymbol{\mathcal{H}}}\,\overline{\boldsymbol{\mathcal{H}}}^\dagger\} + \mathrm{tr}\{\boldsymbol{\mathcal{R}}\} = 1 \tag{4.8}$$

and the 2×2 matrix

$$\mathbf{W}_{n,i} \triangleq \frac{\mu_0 \rho_R}{4} \boldsymbol{\mathcal{R}} \mathbf{F}_{n,i} \mathbf{F}_{n,i}^\dagger \boldsymbol{\mathcal{R}} + \boldsymbol{\mathcal{R}} \tag{4.9}$$

with $\rho_R = \frac{P}{\sigma_w^2}$ being the receive signal to noise ratio (SNR) and P is the average sum receiver power. The 2×2 matrix, $\mathbf{D} \triangleq \mu_0 \mathbf{I}$, is the codeword distance product matrix, which is determined by the minimum distance among all possible codeword pairs [19].

Combined with the power constraint $\mathrm{tr}(\mathbf{F}_{n,i}\mathbf{F}_{n,i}^\dagger) = 1$, the design of the precoder which minimizes the PEP in (4.7) is equivalent to

$$\begin{array}{ll} \min_{\mathbf{F}_{n,i}} & \mathbf{J} = \mathrm{tr}(\overline{\boldsymbol{\mathcal{H}}}\mathbf{W}_{n,i}^{-1}\overline{\boldsymbol{\mathcal{H}}}^{\dagger}) - \log\det(\mathbf{W}_{n,i}) \\ \text{s.t.} & \mathbf{W}_{n,i} = \frac{1}{4}\mu_0\rho_R\boldsymbol{\mathcal{R}}\mathbf{F}_{n,i}\mathbf{F}_{n,i}^{\dagger}\boldsymbol{\mathcal{R}} + \boldsymbol{\mathcal{R}} \\ & \mathrm{tr}(\mathbf{F}_{n,i}\mathbf{F}_{n,i}^{\dagger}) = 1 \end{array} . \tag{4.10}$$

By some transformation and convex optimization techniques in [19], one can obtain the optimal precoder given the channel mean and transmit correlation. The associated PEP upper bound can thus be expressed by

$$\varepsilon(\rho_R, \boldsymbol{\mathcal{R}}, \overline{\boldsymbol{\mathcal{H}}}, \mathbf{F}_{opt}) \tag{4.11}$$

and further more be described by

$$\delta(\rho_R, \boldsymbol{\mathcal{R}}, \overline{\boldsymbol{\mathcal{H}}}) \tag{4.12}$$

which can be computed by only the channel statistics.

Chapter 5

Iterative One-bit Feedback Beamforming Algorithm

Consider the proposed system scheme shown in Fig.5.1. When the LOS path is blocked by some obstructors, STC could exploit the diversity to improve the link quality. Besides, with the low rate feedback link, precoding scheme introduced in previous chapter can further improve the system performance. Besides, HBF architecture is used at the transmitter to combine the RF BF with the mentioned baseband signal processing. In this ST-precoded HBF system scheme, we proposed an iterative one-bit feedback beamforming algorithm to search for the optimal pointing directions with the associated optimal precoder. Besides, along with the beam steering algorithm, a direction-based precoder codebook design criterion for both the transmitter and receiver is proposed to adapt to the channel statistics resulted from different pointing directions.

5.1 Iterative one-bit feedback beamforming algorithm

Assume there is a low rate wireless link for feedback, and the receiver is able to estimate channel mean and transmit covariance matrices for all tones, and knows the design of the precoder given the channel statistics. Consider that the transmission is divided into training phase and data transmission phase. Training phase aims at searching for the optimal pointing directions with the associated optimal precoder while data transmission phase aims at transmitting the data streams. During the training phase,the transmitter keeps recording the pointing directions that results in the best performance so far while the receiver keeping recording the best performance and associated optimal precoder. Let

$$\mathcal{E}^{(r)} \triangleq \frac{1}{N_F}\sum_{n=1}^{N_F}\varepsilon(\rho_R^{(r)}, \boldsymbol{\mathcal{R}}_n^{(r)}, \overline{\boldsymbol{\mathcal{H}}}_n^{(r)}, \mathbf{F}_{n,opt}^{(r)}) \tag{5.1}$$

be the estimated PEP upper bound where $\boldsymbol{\mathcal{R}}_n^{(r)}$ and $\overline{\boldsymbol{\mathcal{H}}}_n^{(r)}$ are the estimates of the transmit correlation and channel mean, respectively, with the corresponding optimal precoder, $\mathbf{F}_{n,opt}^{(r)}$, chosen from the codebook to minimize the PEP upper bound. Besides, the pointing directions of the two BFers, $(\hat{\phi}_1^{(r)}, \hat{\theta}_1^{(r)})$ and $(\hat{\phi}_2^{(r)}, \hat{\theta}_2^{(r)})$, are selected at the r-th iteration. Making use of the estimated PEP upper bound (4.7) as the performance metric at the receiver, the required channel statistics could be obtained by the mentioned Type.I, II and III estimators.

Since the metric of PEP may exist several local maximum values in different transmission directions, local random search methods for direction selection in [8, 29] are not feasible here. Thus, we adopt a global random search method for transmitter to choose the directions. The receiver then chooses the best precoder from the codebooks for current pointing directions and compute the associated PEP upper bound, , after the estima

In the procedure of OBF herein, the directions of the two BFers are chosen uniformly from all adjustable directions and receiver then chooses the best precoder, $\mathbf{F}_{n,opt}^{(r)}$, from the codebooks for current pointing directions and compute the current PEP upper bound, $\mathcal{E}^{(r)}$, after the estimation for $\boldsymbol{\mathcal{R}}_n^{(r)}$ and $\overline{\boldsymbol{\mathcal{H}}}_n^{(r)}$ in each iteration. In this section, we assume the precoder codebooks for both the transmitter are same and given as *a* *priori*. Besides, the receiver records the lowest value of $\mathcal{E}$ obtained so far to $\mathcal{E}^{(0)}$. If $\mathcal{E}^{(r)} \leq \mathcal{E}^{(0)}$ then the receiver feeds back one-bit information, "Good", to the transmitter to update the best directions to $(\hat{\phi}_1^{(r)}, \hat{\theta}_1^{(r)})$ and $(\hat{\phi}_2^{(r)}, \hat{\theta}_2^{(r)})$, otherwise, feeds back one-bit information, "Bad", to keep the old best directions $(\hat{\phi}_1^{(r-1)}, \hat{\theta}_1^{(r-1)})$ and $(\hat{\phi}_2^{(r-1)}, \hat{\theta}_2^{(r-1)})$. The iteration stops when the number of iteration achieves the termination constraint, R. The detailed procedure is shown in Algorithm 1 where $\{(\hat{\phi}_1^{(0)}, \hat{\theta}_1^{(0)}), (\hat{\phi}_2^{(0)}, \hat{\theta}_2^{(0)})\}$ are the feasible directions.

Algorithm 1 One-Bit Beamforming

Rx: $\mathcal{E}^{(0)} \leftarrow 1$
for $r = 1 : R$
    Tx: Choosing $\{(\hat{\phi}_1^{(r)}, \hat{\theta}_1^{(r)}),\ (\hat{\phi}_2^{(r)}, \hat{\theta}_2^{(r)})\}$ randomly
    Rx: Compute $\mathcal{E}^{(r)}$
    if $\mathcal{E}^{(r)} \leq \mathcal{E}^{(0)}$
        $\mathcal{E}^{(0)} \leftarrow \mathcal{E}^{(r)}$, $\mathbf{F}_{n,opt}^{(0)} \leftarrow \mathbf{F}_{n,opt}^{(r)}, n = 1 \ldots N_F$
        Feed a bit "Good" back
    else
        Feed a bit "Bad" back
    end
    Tx:
    if Receive "Good"
    $\{(\hat{\phi}_1^{(0)}, \hat{\theta}_1^{(0)}), (\hat{\phi}_2^{(0)}, \hat{\theta}_2^{(0)})\} \leftarrow \{(\hat{\phi}_1^{(r)}, \hat{\theta}_1^{(r)}), (\hat{\phi}_2^{(r)}, \hat{\theta}_2^{(r)})\}$
    end
end

Note that we assume that both the transmitter and receiver use the same random number generator with the same seed. Thus, the receiver knows which set of point directions is used for BFers currently. The receiver then chooses the best precoder from the codebooks for current pointing directions and compute the associated PEP upper bound, $\varepsilon^{(}r)$, after measuring the channel statistics.

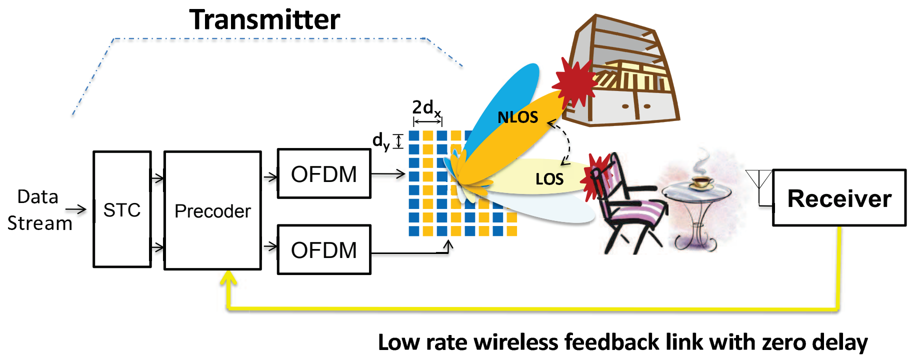

Figure 5.1: Proposed system scheme with ST-precoded HBF architecture and zero-delay low rate wireless broadcasting link.

5.2 Direction-based precoder codebook design criterion

In Section 5.1, we assume the precoder codebook used at both the transmitter and receiver are provided as *a priori*. In this case, to construct the codebook, one may collects all the channel statistics of each tone of each adjustable set of pointing directions at the receiver. The precoder codebook adapting to the associated channel statistics can thus be constructed with the VQ techniques in [28] or GLP procedure in [27]. However, the channel statistics are determined by the pointing direction and indoor environment significantly. Indoor environment may changes every time when there are some obsutructors appearing up in the room or the transmitter and receiver moving which results in the changing of numerous channel statistics. The precoder codebook must be updated at both the transmitter and receiver to adapt to the current channel statistics which raises up the overheads for feedback. Therefore, a precoder codebook design criterion without measuring the channel statistics at the receiver is recommended and essential for the proposed ST-precoded HBF architecture with OFDM system in 60Ghz millimeter wave radio. We herein propose a direction-based precoder codebook design to satisfy this demand.

5.2.1 Direction-based optimal precoder design

Motivated by that although the indoor environment may affect the channel statistics measured at the receiver, there must be some relation between the pointing direction and the channel statistics measured at the receiver according to the multipath environment. Similar considerations appears up in [32]. This research considers the system with a equal spacing linear antenna array in a rich scattering environment where the channel statistics at the transmitter and receiver can be seperated as a form of kronecker product when the LOS path is blocked. The transmit correlation, $\mathbf{R}_t$, can be described by the following exponential correlation model

$$\mathbf{R}_t = \begin{pmatrix} 1 & e^{j\varphi} & \dots & e^{j(n_t-1)\varphi} \\ e^{-j\varphi} & 1 & \ddots & e^{j(n_t-2)\varphi} \\ \vdots & \vdots & \dots & \vdots \\ e^{-j(n_t-1)\varphi} & e^{-j(n_t-2)\varphi} & \dots & 1 \end{pmatrix} \tag{5.2}$$

where φ is a constant phase difference between adjacent antennas. This model motivates the direction-based precoder design. According to the RF beam pattern shown in eq.(2.2). Our purpose is to find the user direction that can support the LOS transmission when the user location is unknown to the transmitter. For a chosen set of pointing directions, we assume the user is located in the pointing directions due to the unknown user location at the transmitter. In this case, when the location of virtual user matches that of the real user, the link quality will be improved. The channel mean of the i-th virtual user, $\overline{\mathbf{h}}_i$, for a chosen set of pointing directions can be expressed by

$$\overline{\mathbf{h}}_i = A^{(1)}(\hat{\phi}_i, \hat{\theta}_i) \begin{bmatrix} 1 & e^{j\alpha_x^{(i)}} \end{bmatrix} \tag{5.3}$$

and the associated transmit correlation, $\mathbf{R}_i$, is given by

$$\mathbf{R}_i = A^{(1)}(\hat{\phi}_i, \hat{\theta}_i)^2 \begin{pmatrix} 1 & e^{j\alpha_x^{(i)}} \\ e^{-j\alpha_x^{(i)}} & 1 \end{pmatrix} \tag{5.4}$$

Moreover, because the precoder design criterion in [19] cannot improve the performance of a NLOS path, we consider the precoding only on the link with high k factor. Therefore, the channel statistics are separated into received snr, $\rho_{R,i}$, normalized channel mean, $\overline{\mathbf{h}}_{i,o}$, normalized transmit correlation, $\mathbf{R}_{i,o}$, and k factor, K, by the following relations

$$\rho_{R,i} = \mathrm{tr}(\overline{\mathbf{h}}_i \overline{\mathbf{h}}_i^\dagger) + \mathrm{tr}(\mathbf{R}_i) \tag{5.5}$$

$$\mathbf{R}_{i,o} = \frac{\mathbf{R}_i / \mathrm{tr}(\mathbf{R}_i)}{\sqrt{\frac{1}{K+1}}} \triangleq \beta(A^{(1)}(\hat{\phi}_i, \hat{\theta}_i), \hat{\phi}_i, \hat{\theta}_i) \tag{5.6}$$

$$\overline{\mathbf{h}}_{i,o} = \frac{\overline{\mathbf{h}}_i / \sqrt{\mathrm{tr}(\overline{\mathbf{h}}_i \overline{\mathbf{h}}_i^\dagger)}}{\sqrt{\frac{1}{K+1}}} \triangleq \gamma(A^{(1)}(\hat{\phi}_i, \hat{\theta}_i), \hat{\phi}_i, \hat{\theta}_i) \tag{5.7}$$

Thus, the optimal precoder corresponding to the channel statistics of i-th virtual user can be determined by the pointing directions in advance for both the transmitter and receiver at each iteration of the OBF procedure. The associated PEP upper bound for i-th virtual can thus be expressed by

$$\delta(\rho_R, \boldsymbol{\mathcal{R}}, \overline{\boldsymbol{\mathcal{H}}}) = \delta(\rho_R, K, \mathbf{R}_{i,o}, \overline{\mathbf{h}}_{i,o}) \tag{5.8}$$

Each set of pointing directions consist of two pointing directions which results to two virtual user locations resulting in two corresponding optimal precoders. Such precoding design method is called direction-based optimal precoder design criterion.

5.2.2 Direction-based precoder codebook design

Considering that the environment may affect the channel statistics resulted from the pointing directions and user direction may not exactly be located in the adjustable pointing directions. For the i-th virtual user of a chosen set of pointing directions, there are $N_\phi \times N_\theta$ spreading precoder codewords designed by the spreading normalized channel mean, $\tilde{\overline{\mathbf{h}}}_{i,(n_\phi,n_\theta)}$, and spreading normalized transmit correlation, $\tilde{\mathbf{R}}_{i,(n_\phi,n_\theta)}$, defined by

$$\tilde{\mathbf{R}}_{i,(n_\phi,n_\theta)} = \beta(A^{(1)}(\tilde{\phi}_{i,n_\phi}, \tilde{\theta}_{i,n_\theta}), \tilde{\phi}_{i,n_\phi}, \tilde{\theta}_{i,n_\theta}) \tag{5.9}$$

$$\tilde{\overline{\mathbf{h}}}_{i,(n_\phi,n_\theta)} = \gamma(A^{(1)}(\tilde{\phi}_{i,n_\phi}, \tilde{\theta}_{i,n_\theta}), \tilde{\phi}_{i,n_\phi}, \tilde{\theta}_{i,n_\theta}) \tag{5.10}$$

where the spreading azimuth angle, $\tilde{\phi}_{i,n_\phi}$ and spreading elevation angle, $\tilde{\theta}_{i,n_\theta}$, are determined by a set of angular spread centralized in the i-th pointing direction which can be expressed by

$$\begin{aligned} \tilde{\theta}_{i,n_\theta} &\in \{\hat{\theta}_i \pm \tfrac{n_\theta \times (\frac{\pi}{4})}{N_\theta}\} \quad, n_\theta = 1, 2, \ldots, \frac{N_\theta}{2} \\ \tilde{\phi}_{i,n_\phi} &\in \{\hat{\phi}_i \pm \tfrac{n_\phi \times (\frac{\pi}{8})}{N_\phi}\} \quad, n_\phi = 1, 2, \ldots, \frac{N_\phi}{2} \end{aligned} \tag{5.11}$$

where N_ϕ is the number of spreading azimuth angle and N_θ is the number of spreading elevation angle. In this case, for the chosen set of pointing directions at r-th iteration of the OBF procedure, we define the set of k factor codewords, normalized transmit correlation codewords and normalized channel mean by $\Sigma_K^{(r)}$, $\Sigma_R^{(r)}$ and $\Sigma_{\overline{\mathbf{h}}}^{(r)}$ respectively.

5.2.3 Codeword selection

After measuring the channel statistics of received SNR, $\rho_R^{(r)}$, k factor, $K_{measured}^{(r)}$, normalized transmit correlation, $\mathbf{R}_{measured}^{(r)}$, and normalized channel mean, $\overline{\mathbf{h}}_{measured}^{(r)}$, at r-th iteration of the OBF procedure, the receiver will choose the precoder codeword design by the channel statistics with the indexes, $\{K_{opt}^{(r)}, \mathbf{R}_{opt}^{(r)}, \overline{\mathbf{h}}_{opt}^{(r)}\}$, resulting in the best performance in PEP upper bound from the codebook corresponding to r-th set of pointing directions. Selection for the best k factor, normalized transmit correlation and normalized channel mean are determined by

$$K_{opt}^{(r)} = \underset{K_a \in \Sigma_K^{(r)}}{arg\min} \|K_a - K_{measured}^{(r)}\| \tag{5.12}$$

$$\{\mathbf{R}_{opt}^{(r)}, \overline{\mathbf{h}}_{opt}^{(r)}\} = \underset{\mathbf{R}_b \in \Sigma_R^{(r)}, \overline{\mathbf{h}}_c \in \Sigma_{\overline{\mathbf{h}}}^{(r)}}{arg\min} \varepsilon(\rho_R^{(r)}, K_{measured}^{(r)}, \mathbf{R}_{measured}^{(r)}, \overline{\mathbf{h}}_{measured}^{(r)}, \mathbf{F}_{opt}) \tag{5.13}$$

where the optimal precoder is computed by the channel statistics.

Chapter 6

Simulations

We present some simulation results to verify the performance of the proposed ST-precoded HBF scheme with the proposed beam steering algorithm for 60GHz radio. In particular, we consider the environment of an indoor conference room whose length, width and height are 9 , 9 and 5 meters, respectively. The transmitter and the receiver are both located on desks with 1 meter above the ground shown in Fig.6.1. The bandwidth is equal to 1Ghz, and σ_w^2 is taken form the thermal noise with the temperature at $25^o C$. Therefore, the power of thermal noise is equal to -77.8 dbm, that is, transmit power is equal to 0 dbm when transmit SNR is equal to 77.8 db. The number of the frequency tones for OFDM is $N_F = 1024$, and the CP ratio is equal to $1/4$. QPSK is used for symbol modulation. Besides, three sets of pointing directions are chosen to look into the performances of the proposed scheme for the LOS and NLOS transmissions. Direction 1 corresponds to LOS transmission, while in direction 2, only one of the two BFers has a LOS transmission to the receiver. Direction 3 is for NLOS transmission. The details of the channel characteristics for these three directions are listed in Table.6.1.

Fig. 6.2 and Fig. 6.3 shows the simulation results in the environment without obstructions, or so called LOS blockage, in the LOS path. Fig. 6.2 compares the PEP upper bounds defined in (5.1) between LOS and NLOS transmissions, and without and

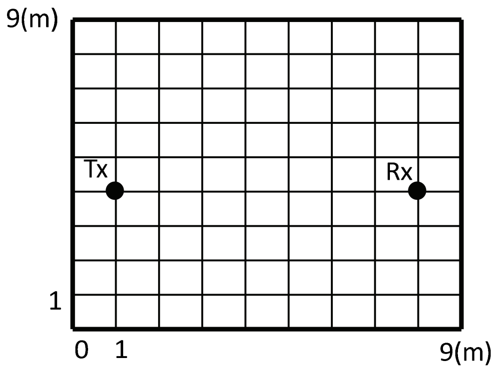

Figure 6.1: Location of the transmitter and receiver for simulations.

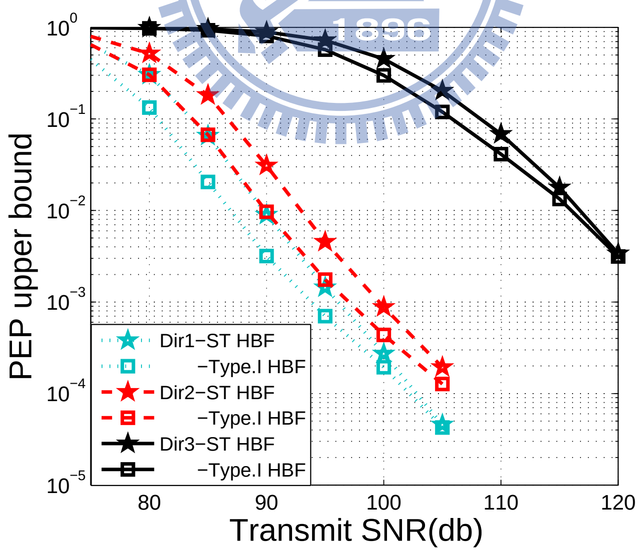

Figure 6.2: PEP upper bounds versus transmit SNR using Type I statistics .

Table 6.1: Channel statistics of different transmission directions.

Direction index (Dir)	1	2	3
K-factor	4.7	4.65	1.3×10^{-30}
Channel power (db)	-62.2	-65.2	-82.7

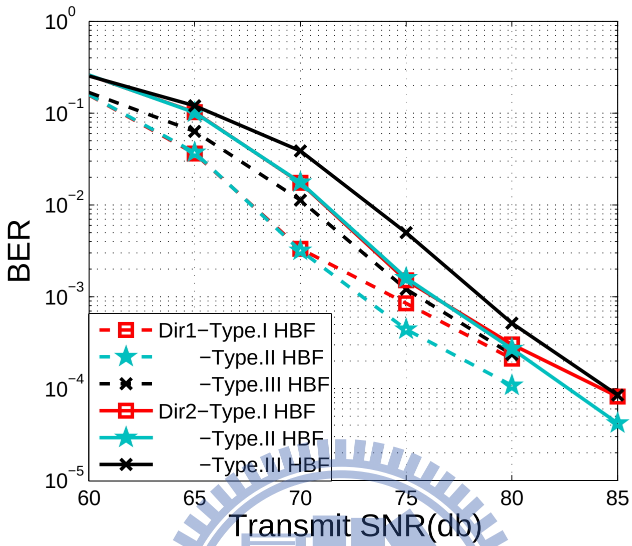

Figure 6.3: BERs versus transmit SNR using Type I, II and III statistics .

with the precoders formed based on the Type I statistics. As shown in the figure, the LOS transmission can provide significant SNR gain over the NLOS transmission. Besides, precoding further improves the performance of LOS transmissions. This demonstrates the performance of the ST-precoded HBF in 60GHz radio. Fig. 6.3 shows the BERs with Type I, II and II statistics. For direction 1, 62.2 db transmit SNR is equals to 0 db received SNR. Apparently, we can use Type II statistics to reduce the time to acquire the channel statistics as well as the complexity in precoder designs as there is no need to use different precoders for different frequency tones. Moreover, the performance loss without considering the transmit correlation is a modicum in this 2×1 MISO system, which can further reduce the complexity in precoder designs. Fig. 6.4 compares the BERs between the environments with and without LOS blockage. The solid lines are simulated in the environment where the LOS path is blocked. The curves with square and star marks

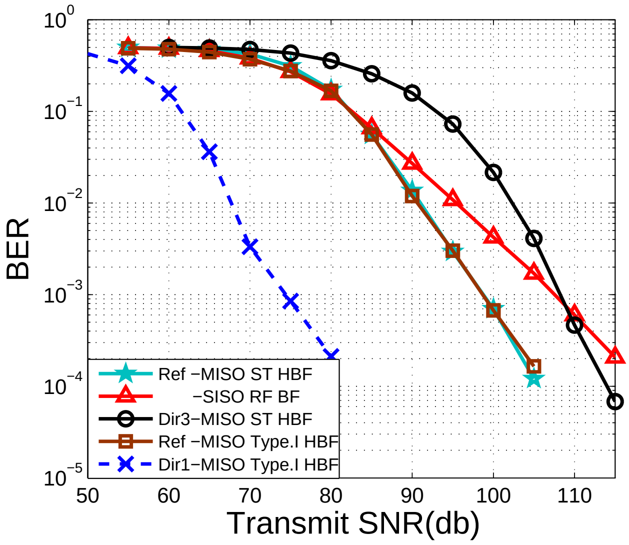

Figure 6.4: BER comparisons between the ST-precoded HBF and the RF BF in the environments with and without LOS blockage.

correspond to the BERs of 2×1 MISO systems using the ST-precoded HBF with and without precoding when the transmit BFer of each block of the PAA is pointed to the best reflectional directions to the receiver. In contrast, the curve with triangle marks is the BER of a SISO system using the RF BF only with an 8×8 PAA when its BFer is also pointed to the best reflectional direction to the receiver. Apparently, the channel diversity with HBF is greater than that of the RF BF even if the antenna gain of the SISO system is greater than that of each block in the MISO system. This justifies the use of the MISO HBF with PAA in 60 GHz radio. Besides, precoders designed by the criterion we adopt in [19] cannot improve the performance in BER when the LOS path is blocked. The dashed curve with cross marks corresponds to LOS transmission in the environment without LOS blockage. It is obviously that the obstructions in the LOS path degrade the performance in BER significantly.

Finally, the convergence curves of the PEPs of the proposed OBF algorithm are shown in Fig. 6.5 in comparison with that of the LOS transmission in the environment without LOS blockage. The precoders are formed with the Type I estimators and the transmit SNR is 95dB. The curves with no marks corresponding to LOS transmission in the environment without LOS blockage while the curves in brown with triangle marks represent the performance of proposed OBF algorithm without the utilization of precoder book. Besides, the curves in red color with cross marks denote the performance of proposed OBF algorithm with the utilization of precoder codebook in which there are no spreading codewords while the curves with square marks correspond to that with the utilization of precoder codebook in which there are $N_\phi \times N_\theta$ spreading codewords where the numbers of spreading codewords are set to $2 \times 2 = 4$. As shown in the figure, the PEP metric of OBF algorithm with the optimal precoder converges close to that of the LOS transmission when the number of iterations is greater than 15 which is $19.2\mu s$ and is much smaller than that of using the exhaustive search out of the set defined in (2.3). Therefore, the proposed OBF algorithm significantly reduces the time in searching the directions for the RF BFers. Besides, The performance difference between the OBF algorithm with and without the proposed direction-based precoder codebook are just a modicum as the SNR becomes larger. The direction-based precoder codebook is suitable for the 60Ghz millimeter wave radio with the proposed ST-precoded HBF scheme.

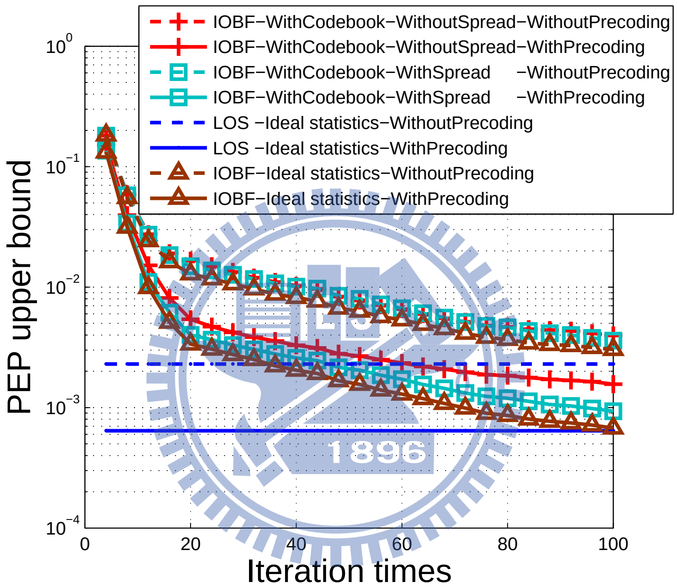

Figure 6.5: Convergence analysis of the iterative OBF BF algorithm.

Chapter 7

Conclusions

We studied a ST-precoded HBF architecture for broadband transmissions in 60GHz radio using PAA. Under the hybrid PAA architecture, a 2×1 ST precoded HBF scheme can provide a 2$\sim$ 4dB SNR gain in LOS transmissions, where the LOS path isn't blocked, compared with a PAA architecture using the RF BF only. In addition, an efficient OBF BF scheme is proposed to search for the optimal directions of the RF BFers to support LOS transmissions in 60GHz radio. Simulation results show that the OBF scheme converges closed to the LOS transmission in 100 iterations which is much more efficient than exhaustively searching for the directions for RF BFers without the quantization of precoder. Besides, we proposed a direction-based precoder codebook design criterion to provide the precoder codebook for both the transmitter and receiver as *a priori*. Simulation results show that the performances between the OBF algorithm with and without the quantization of optimal precoder utilizing the proposed precoder codebook is just a modicum which makes the proposed direction-based precoder codebook design method feasible for the proposed ST-precoded HBF system scheme in 60Ghz millimeter wave radio.

Chapter 8

APPENDIX

8.1 APPENDIX A

8.2 APPENDIX B

8.3 APPENDIX C

Bibliography

[1] "IEEE 802.15 WPAN Millimeter Wave Alternative PHY Task Group (TG3c)," available at http://www.ieee802.org/15/pub/TG3c.html.

[2] C. R. Anderson and T. S. Rappaport, "In-building wideband partition loss measurements at 2.5 and 60 GHz," *IEEE Trans. on Communications*, vol. 3, no. 3, pp. 922–928, May 2004.

[3] "IEEE 802.11ad: Very High Throughput 60 GHz," available at http://www.ieee802.org/11/.

[4] WirelessHD, "http://www.wirelesshd.org/index.html,," .

[5] David M. Pozar, "Microstrip Antennas," *Proceedings of the IEEE*, vol. 80, no. 1, pp. 79 – 91, Jan. 1992.

[6] E. Suematsu A. Yamada, Y. Amano and H. Sato, "A patch antenna array on a multi-layered ceramic substrate for 60 GHz applications," *Proc. European Microwave Conference*, vol. 15, no. 5, pp. 339 – 341, May. 2005.

[7] Chang-woo Pyo Baykas T. Chin-sean Sum Rahman M.A. Jing Gao Funada R. Kojima F. Harada H. Kato S. Junyi Wang, Zhou Lan, "Beam codebook based beamforming protocol for multi-Gbps millimeter-wave WPAN systems," *IEEE Journal on Selected Areas in Communication*, vol. 27, no. 8, pp. 1390 – 1399, Oct. 2009.

[8] U. Madhow R. Mudumbai, B. Wild and K. Ramchandran, "Distributed beamforming using 1 bit feedback: from concept to realization ," *in Proc. of 44th Allerton Conf. on Commun. Control and Comput.*, pp. 1020–1027, Sept. 2006.

[9] J. Thukral and H. Bolcskei, "Distributed spatial multiplexing with 1-bit feedback," *in Proc. of 45th Allerton Conference on Communication, Control, and Computing*, pp. 502–509, Sept. 2007.

[10] S.-S. Wu, L.-K. Chiu, K.-Y. Lin, and S.-J. Chung, "Planar arrays hybrid beamforming for SDMA in millimeter wave applications," in *IEEE PIMRC.* Cannes, France, 15-18 Sep. 2008.

[11] Y. Jay Guo X. Huang and J. D. Bunton, "A hybrid adaptive antenna array," *IEEE Trans. on Wireless Communications*, vol. 9, no. 5, pp. 1770 – 1779, May. 2010.

[12] S.-S. Wu, K.-Y. Lin, and L.-K. Chiu, "Hybrid Beamforming for Two-User SDMA in Millimeter Wave Radio," in *IEEE PIMRC.* Instanbul, 26-30 Sept. 2010.

[13] S . M. Alamouti, "A simple transmit diversity techniquefor wirelss communication," *IEEE Journal on Selected Areas in Communication*, vol. 16, pp. 1451–1458, Oct. 1998.

[14] P. F. M. Smulders, "Statistical characterization of 60-GHz indoor radio channels," vol. 57, no. 10, pp. 2820 – 2829, Oct. 2009.

[15] S. Zhou, , and G. B. Giannakis, "Optima transmitter eigen-beamforming and space-time block coding based on channel mean feedback," *IEEE Trans. on Signal Processing*, vol. 50, no. 10, pp. 2599 – 2163, Oct. 2002.

[16] S. Zhou, , and G. B. Giannakis, "Optimal transmitter eigen-beamforming and space-time block coding based on channel correlations," *IEEE Trans. on Information Theory*, vol. 49, no. 7, pp. 1673 – 1690, July. 2003.

[17] H. Sampath and A. Paulraj, "Linear precoding for space-time coded systems with known fading correlations," *Signals, Systems and Computers, 2001. Conference Record of the Thirty-Fifth Asilomar Conference on*, vol. 1, pp. 246 – 251, 2001.

[18] S. Zhou, , and G. B. Giannakis, "Application of quasi-orthogonal space-time block codes in beamforming," *IEEE Trans. on Signal Processing*, vol. 53, no. 1, pp. 54 – 63, Jan. 2005.

[19] M. Vu and A. Paulraj, "Optimal Linear Precoders for MIMO Wireless Correlated Channels With Nonzero Mean in Space-Time Coded Systems," *IEEE Trans. on Signal Processing*, vol. 54, no. 6, pp. 2318–2332, Mar. 2005.

[20] M. Vu and A. Paulraj, "MIMO wireless linear precoding," *IEEE Signal Processing Mag.*, vol. 24, no. 5, pp. 86 – 105, Sept. 2007.

[21] U. Torkildson, E.; Hong Zhang; Madhow, "Channel modeling for millimeter wave MIMO," *Information Theory and Applications Workshop*, pp. 1 – 8, Jan. 2010.

[22] Z. Wang and G. B. Giannakis., "Linearly precoded or coded OFDM against wireless channel fades?," *Proc. 3rd IEEE Workshop Signal Process. Adv. Wireless Commun.*, pp. 267 – 270, Mar. 2001.

[23] K. Kusume, "Linear space-time precoding for OFDM systems based on long-term CSI," *IEEE PIMRC*, vol. 2, pp. 949 – 953, 2004.

[24] H. Yang, P. F. M. Smulders, and M. H. A. J. Herben, "Channel characteristics and transmission performance for various channel configurations at 60 GHz," *EURASIP Journal on Wireless Communications and Networking*, to appear.

[25] M. Meurer T. Weber C. A. Jotten, P. W. Baier and M. Haardt, "Efficient representation and feedback signaling of channel state information in frequency division

duplexing MIMO systems," *Proc. IEEE Int. Symp. Wireless Personal Multimedia Commun.*, vol. 2, pp. 444 – 448, Oct. 2002.

[26] Y. Liu W. Dai and B. Rider, "Quantization bounds on Grassmann manifolds and applications to MIMO communications," *IEEE Trans. on Information Theory*, vol. 54, no. 3, pp. 1108 – 1123, Mar. 2008.

[27] Jr. David J. Love, Robert W. Heath, "Grassmannian beamforming on correlated MIMO channels," *Proc. IEEE GLOBECOM'04*, vol. 1, pp. 106 – 110, Dec. 2004.

[28] Akbar M. Sayeed Vsanthan Raghavan, Venugopal V. Veeravalli, "Quantized Multimode Precoding in Spatially Correlated Multi-Antenna Channels," *IEEE Trans. on Signal Processing*, vol. 56, no. 12, pp. 6017 – 6030, Dec. 2008.

[29] V. V. Veeravalli C. Lin and S. P.Meyn, "A random search framework for convergence analysis of distributed beamforming with feedback," *IEEE Trans. on Information Theory*, vol. 56, no. 12, pp. 6133–6141, Dec. 2010.

[30] C. A. Balanis, *Antenna Theory*, John Wiley & Sons, 2 edition, 1997.

[31] H. Ochiai P. Mitran and V. Tarokh, "Space-time diversity enhancements using collaborative communications," *IEEE Trans. on Information Theory*, vol. 50, no. 6, pp. 2041– 2057, June 2005.

[32] C. Martin and B. Otterstenm, "Asymptotic eigenvalue distributions and capacity for MIMO channels under correlated fading," *IEEE Trans. on Wireless Communications*, . 2004.